



# The role of plant input physical-chemical properties, and microbial and soil chemical diversity on the formation of particulate and mineral-associated organic matter

M. Francesca Cotrufo <sup>a,b,\*</sup>, Michelle L. Haddix <sup>a,b</sup>, Marie E. Kroeger <sup>c</sup>, Catherine E. Stewart <sup>d</sup>

<sup>a</sup> Department of Soil and Crop Sciences, Colorado State University, Fort Collins, CO, USA

<sup>b</sup> Natural Resource Ecology Laboratory, Colorado State University, Fort Collins, CO, USA

<sup>c</sup> Bioscience Division, Los Alamos National Laboratory, Los Alamos, NM, USA

<sup>d</sup> Soil Management and Sugarbeet Research Unit USDA-Agricultural Research Service, Fort Collins, CO, USA



## ARTICLE INFO

### Keywords:

Litter decomposition  
Soil organic matter  
Chemical diversity  
Microbial diversity  
Mineral-associated organic matter  
Particulate organic matter

## ABSTRACT

Soil organic matter (SOM) is a fundamental resource to humanity for the many ecosystem services it provides. Increasing its stocks can significantly contribute to climate change mitigation and the sustainability of agricultural production. Elucidating the mechanisms and drivers of the formation of the main components of SOM, particulate (POM) and mineral associated (MAOM) organic matter, from the decomposition of plant inputs is therefore critical to inform management and policy designed to promote SOM regeneration. We designed a two-tiered laboratory incubation experiment using <sup>13</sup>C and <sup>15</sup>N labeled plant material to investigate the effects of the physical nature (i.e., structural versus soluble) of plant inputs as well as their chemical composition on (1) the pathways of SOM formation, (2) the soil microbial community and chemical diversity, and (3) their interaction on the stabilization efficiency of litter-derived C in POM and MAOM, in a topsoil and a subsoil. We found that: i) the physical nature of the plant input (structural vs soluble) drove both the pathways and efficiencies of SOM formation; ii) POM formation from the decomposition of structural residues increased in efficiency the more decomposed were the residues, and linearly with soil microbial and chemical diversity, the latter only for subsoil; iii) more input-derived C and N were retained in subsoil because of both higher stabilization in MAOM and POM, and slower residue decay. Our results also confirm the importance of direct sorption of soluble inputs to silt- and clay-sized minerals for the formation of MAOM in bulk soils. Taken together these finding suggest that the highest potential for SOM accrual is in subsoils characterized by higher C saturation deficit, from the separate addition of decomposed residues and soluble plant inputs.

## 1. Introduction

Soil organic matter (SOM) provides critical ecosystem services (Smith et al., 2015) and is at the nexus of some of the major challenges facing humanity, including mitigating climate change and sustaining food and fiber production. Thus, preserving and increasing current SOM stocks is a critical humanity goal (Amundson et al., 2015; Keesstra et al., 2016). SOM content has declined in managed soils over the millennia of human land use (Sanderman et al., 2017). There is a large opportunity to promote conservation agricultural practices to halt this loss and build new SOM in managed landscapes. Yet, it is imperative, that such practices do not result in increased N<sub>2</sub>O emissions (Guenet et al., 2021).

SOM is not made equal, and at a minimum it's important to

understand what controls accrual of its distinct components: particulate (POM) and mineral-associated organic matter (MAOM) if we strive to provide meaningful guidance for regenerative SOM management (Lavallee et al., 2020). Advances have been made in recent years towards elucidating the mechanisms and controls of POM and MAOM formation (Cotrufo and Lavallee 2021), yet alternative hypotheses have been proposed which need further testing. Typically, SOM is considered to form from the continuous depolymerization of polymeric plant inputs, which once in the mineral soil are defined POM. The depolymerization of POM, which is slowed down if it is occluded in aggregates, produces lower molecular weight products, which are either mineralized to CO<sub>2</sub> through microbial catabolism, or stored in MAOM by association to minerals (Grandy and Neff 2008; Lehmann and Kleber 2015). In

\* Corresponding author. 200 W. Lake street, Fort Collins, CO, 80523-1170, USA.

E-mail address: [Francesca.cotrufo@colostate.edu](mailto:Francesca.cotrufo@colostate.edu) (M.F. Cotrufo).

contrast, Cotrufo et al. (2015) proposed two distinct pathways for POM and MAOM formation from the decomposition of different plant components. In particular, dissolved organic matter (DOM) inputs produced from plant exudates, the leaching of water-soluble components of plant residues, or from the depolymerization of easily degradable polymers (e.g. neutral and acid hydrolysable fibers) are expected to form MAOM via direct sorption when the probability to encounter a mineral surface is higher than to encounter a microbial cell (Sokol et al., 2019), or after *in vivo* microbial transformation, and the association of microbial products to minerals (Kleber et al., 2015; Liang et al., 2017). On the other hand, POM is expected to form from the fragmentation of partially decomposed more chemically recalcitrant polymeric structures (e.g., acid unhydrolyzable fibers) predominantly of plant origin (Cotrufo et al., 2015). Additionally, because of the low microbial carbon use efficiency of chemically recalcitrant (i.e., acid unhydrolyzable) fibers, little MAOM formation is expected from the decomposition of highly decomposed structural litter residues and POM (Cotrufo et al., 2013). While these hypotheses have found some confirmation both in laboratory (Haddix et al., 2016), and field studies (Haddix et al., 2020), somewhat contrasting results have also been observed (Córdova et al., 2018), further testing in contrast to the continuous model (Lehmann and Kleber 2015) is warranted.

In addition to the models of formation, the factors controlling the stabilization efficiency of the newly formed SOM, defined as the proportion of carbon stored in SOM (or its component fractions) of the carbon lost through decomposition (Castellano et al., 2015; Lavallee et al., 2018) also requires investigation. Traditionally it was thought that the higher the proportion of acid unhydrolyzable fraction in plant inputs the more SOM would form (Berg and McClaugherty 2008). More recently, it was proposed that SOM is best described by POM and MAOM (Cambardella and Elliott, 1992; Lavallee et al., 2020), and that while POM and MAOM both span a range of mean residence times with significant overlaps (Cotrufo and Lavallee 2021; Heckman et al., 2021), MAOM stores the most persistent and less vulnerable fraction of carbon in SOM (von Lutzow et al., 2006; Rocci et al., 2021), and in agricultural land also the largest amount (Lugato et al., 2021). Thus, their stabilization efficiency needs to be studied independently.

The relative importance of microbial and inherent plant chemical traits for the efficiency of MAOM formation is under debate. Soluble, chemically labile compounds can result in more efficient MAOM formation due to their affinity to bond to mineral surfaces (Kleber et al., 2015), and because microbes can use them with high efficiency, and microbial products can subsequently associate to minerals (Cotrufo et al., 2013; Kallenbach et al., 2016). Few studies (Bonner et al., 2018; Domeignoz-Horta et al., 2021; Ernakovich et al., 2021) investigated the role of microbial diversity on the decomposition of residues and the subsequent stabilization efficiency of SOM. They suggest that microbial diversity may have a role, but its effect on MAOM formation depends on land-cover (Ernakovich et al., 2021). Lehmann et al. (2020) proposed that decomposition is driven by the molecular diversity of the organic substrates more than their physical properties (e.g., soluble *versus* structural). According to this view, chemical diversity increases with residue decomposition and the contribution of microbial products to SOM, thus decreasing the energy return on investment of SOM mineralization and resulting in its preservation. We posit here that independent of whether it is the physical property, the chemical diversity of plant inputs or both to control their decomposition and the stabilization efficiency of newly formed SOM, microbial diversity is also a key driving factor, in particular of MAOM formation.

MAOM formation efficiency is also expected to be determined by the soil matrix stabilization capacity (Cotrufo et al., 2013). In fact, while POM may accumulate with no apparent upper limits, MAOM requires available mineral surfaces to form and therefore its accumulation may saturate (Six et al., 2002; Stewart et al. 2007, 2008b; Cotrufo et al., 2019). Therefore, soils with higher C saturation deficit may be predicted to have higher stabilization efficiencies (Stewart et al., 2007; 2008a).

While large geographical scale field experiments will be required to prove these concepts, mechanistic laboratory experiments are needed to elucidate specific mechanisms and test this set of hypotheses.

The aim of this study was to determine (1) SOM formation pathways from plant inputs of differing physical (soluble vs. structural) and chemical properties, (2) how these properties modify the soil chemical composition and microbial diversity, and (3) the effects of plant inputs physical properties, and soil chemical and microbial diversity on the stabilization efficiencies of litter-derived C in POM and MAOM, in a topsoil and a subsoil with contrasting C saturation deficit and microbial abundance.

We hypothesized that soluble plant inputs, such as litter leachates, would efficiently result in the formation of MAOM, while structural litter residues would preferentially form POM, in particular residues at advanced stages of decomposition. In accordance with the functional complexity framework (Lehmann et al., 2020), we hypothesized that, independent of their physical structure, litter inputs with higher chemical diversity would increase the microbial diversity of soils and result in higher overall soil chemical diversity, and accumulation of litter input-derived SOM. Specifically, we expected microbial diversity to promote MAOM stabilization efficiency, and plant input chemical diversity to promote POM stabilization efficiency. Because subsoils typically have lower microbial abundance (Taylor et al., 2002), but higher carbon saturation deficit than topsoils (Stewart et al., 2008; Chen et al., 2018), we expect litter decomposition and SOM formation to differ between them. In particular, because of the low microbial but high mineral surface abundance we expect subsoil to have more efficient MAOM formation from the direct sorption of soluble litter components (i.e., leachates) to minerals (Sokol et al., 2019), but also to have higher POM formation from the slower decomposition of structural litter residues, than topsoil.

To test these hypotheses, we performed a two-stage laboratory experiment. First, to produce traceable litter inputs of different physical structure and chemical properties but of the same plant species, we incubated  $^{13}\text{C}$  and  $^{15}\text{N}$  labeled sorghum leaves in leachate cups (Soong et al., 2015) and periodically harvested the leachates and litter over the course of one year. The isotopically labeled residues at various stages of decomposition were characterized for their chemical properties and physical structures, and then added into a topsoil and subsoil, characterized by contrasting chemical and microbial complexity, and incubated for another year. During which time the  $^{13}\text{C}-\text{CO}_2$  respiration was measured from each soil-litter unit. After a year, the remaining litter was picked out, and the soil analyzed for microbial community  molecular composition, and SOM fractionated by size and density. Using the isotope tracer, we identified the litter input derived C and N forming POM and MAOM and related the stabilization efficiencies to the initial litter chemical-physical properties, and the chemical and microbial diversity of soils.

## 2. Materials and methods

### 2.1. First labeled litter incubation

For this experiment, we used leaves from *Sorghum bicolor v. BTx 623* grown in pots for 22 weeks in a  $^{13}\text{C}$  and  $^{15}\text{N}$  continuous labeling chamber, as described in Fulton-Smith and Cotrufo (2019). At harvest, above ground material was cut at the base of the plants, and leaves stripped from the stalks by hand, mixed to make a well homogenized sample and air dried before used for the laboratory incubation. Additionally, a subsample was set aside for chemical analyses as described below.

For the incubation, leaves were cut into 1 cm pieces and incubated in leaching cups with 20  $\mu\text{m}$  nylon filter placed within 3.8 L jars fitted with septa with water in the bottom of the jar to maintain humidity, as described by Soong et al. (2015). One milliliter of soil inoculant was added to each cup at the start of the incubation. The inoculant was made from 1 g of soil from a clay loam soil grown with sorghum at the

Agricultural Research Development and Education Center, Colorado, USA, added to 100 mL of deionized water and shaken for 2 h. The soil was then allowed to settle, and the solution filtered through a 20 µm nylon filter. There were 12 replicates of each harvest point (14 days, 6 months, and 12 months) and 1.5–3 g of litter were incubated, depending on when the cup was going to be harvested to assure to obtain enough material at harvest for the second incubation experiment (described below). Litter was incubated in the dark in a constant temperature room at 25 °C. Respiration was measured daily, then weekly, and then monthly over the incubation using a Li-COR Gas Hog IRGA (Li-COR Biosciences, Lincoln, NE, USA). After the respiration was measured, cups were leached with 30 mL of deionized water and leachates measured for total organic C and total N using a Shimadzu TOC-L/TNM-L Analyzer (Shimadzu Corporation, Kyoto, Japan). The leachates collected during the first 14 days incubation were consolidated and frozen to be used for the second incubation. At each harvest point the litter was removed from jars, allowed to air dry and the twelve replicates were combined randomly into four replicates for chemical analysis and the second incubation.

## 2.2. Second labeled litter and litter leachates incubation in soil

The sorghum fresh litter (FL), the litter leachates (LL) produced during the first 14 days of incubation, and the litter residues collected after 14 day (LR<sub>14d</sub>), 6 months (LR<sub>6m</sub>) and 12 months (LR<sub>12m</sub>) of decomposition during the first incubation described above, were used for this second incubation.

Litters and leachates were incubated in two soils. To provide a range in soil C levels, we used well-characterized topsoil (0–10 cm) and subsoil (120–150 cm) from a long-term bioenergy study at the University of Nebraska's Eastern Nebraska Research and Extension Center (ENREC) (latitude 41.151, longitude 96.40) in Saunders County, 50 km west of Omaha, NE [details in [Stewart et al. \(2016\)](#)]. The soils were sampled in 2014 from continuous no-tillage residue retained plots with typical N fertilizer addition, 180 kg N ha<sup>-1</sup>. These soils were chosen because they had the desired contrast in C content (1.93% C topsoil; 0.29% C subsoil) and texture (6.3% sand topsoil, 2.1% sand subsoil), as well as in microbial abundance (DNA was 5.5 ± 0.26 ng/µL in topsoil, and 0.5 ± 0.036 ng/µL in the subsoil for the control treatment by the end of the incubation), while being within the same soil type.

For this second incubation, 35 g of air-dry soil was mixed with 0.7 g of air-dried litter (FL, LR<sub>14d</sub>, LR<sub>6m</sub>, LR<sub>12m</sub>), or 3.25 mL of litter leachate (LL), equivalent to 7.8 mg of C, following litter addition rates used in [Haddix et al. \(2016\)](#), along with a no litter control (0 L) within 120 mL plastic cups. The experiment thus consisted in a total of six litter types: 0 L, FL, LL, LR<sub>14d</sub>, LR<sub>6m</sub>, LR<sub>12m</sub>, and two soil types: topsoil (0–10 cm), and subsoil (120–150 cm), in a fully factorial design with four replicates. Cups were placed in 1 L jars fitted with septa with water in the bottom of the jar to maintain humidity. Soils were maintained at 50% water filled pore space ([Linn and Doran 1984](#)) and incubated in the dark in a constant temperature room at 25 °C.

During the one year of incubation, CO<sub>2</sub> was measured daily, then weekly, and later monthly, as described above. After each CO<sub>2</sub> measurement, jars were flushed with CO<sub>2</sub> free air and re-sealed. Measurements for δ<sup>13</sup>C-CO<sub>2</sub> were done every other CO<sub>2</sub> measurement on a GV-Optima dual inlet stable isotope mass spectrometer (GV Instruments, Manchester, UK). After one year, all the jars were harvested and the soil was sieved through a 2 mm sieve, litter residues on the sieve were picked out, a 10 g subsample was frozen at -80 °C for subsequent microbial analyses, while the remaining soil was air-dried. The litter residues were oven dried at 105 °C and ashed in a muffle furnace at 600 °C for 5 h to correct for soil contamination and determine the amount of litter mass remaining after the incubation.

## 2.3. Chemical-physical analyses of litter

Fresh litter and litter residues obtained from the first incubation experiment were characterized for their C and N concentration and isotopic composition by elemental analyses isotope ratio mass spectrometry (EA-IRMS), and for their chemical structure and composition by wet chemistry and pyrolysis gas chromatography-mass spectrometry (py-GC/MS).

A subsample of each litter type (FL, LR<sub>14d</sub>, LR<sub>6m</sub>, LR<sub>12m</sub>) was pulverized and oven dried at (60 °C) and the LL was freeze dried prior to analyses of %C, %N, δ<sup>13</sup>C and δ<sup>15</sup>N on a Costech elemental combustion system coupled to a Thermo Scientific Delta V Advantage Isotope Ratio Mass Spectrometer.

To determine the amount of hot water extractable (HWE) compounds, a sub sample (0.35 g) of air-dried material, for each of the four litter residue types (FL, LR<sub>14d</sub>, LR<sub>6m</sub>, LR<sub>12m</sub>) was added to 40 mL of hot, deionized water in a covered test tube and kept in a digestion block at 100 °C for 3 h. HWE were then separated from the residue by pouring the samples over a 20 µm nylon filter ([Soong et al., 2015](#)). Extracts were analyzed for organic C and N using a TOC analyzer (Shimadzu TOC 5000, Shimadzu Scientific Instruments, Inc.).

We used the acid detergent fiber digestion method ([Goering and Van Soest, 1970](#)) to quantify and characterize the litter structural components. A subsample (0.3 g) of each litter type was first digested in Cetyl trimethylammonium bromide (CTAB) and sulfuric acid to remove hemicellulose and other non-structural carbohydrates and lipids, which were quantified as neutral hydrolyzable fraction (NHF). Next, samples were digested in 73% sulfuric acid to remove the acid hydrolyzable fraction (AHF) and collect the acid-unhydrolyzable fraction (AUF). Residues of the hot water extraction and acid digestion were dried overnight at 105 °C prior to weighing. The AUF fraction was subsequently ashed in a muffle oven, for ash-free mass determination. AHF is used as a proxy for celluloses ([McKee et al., 2016](#)), while AUF as a proxy for lignin, but it may also contain waxes, cutin, suberin, and condensed tannins ([Preston and Trofymow, 2015](#)). We calculated the lignocellulose index (LCI) as the ratio between AUF and total fibers [LCI = AUF/(AUF + AHF)] ([Soong et al., 2015](#)).

To obtain a characterization of the chemical properties and diversity of the litters, we used pyrolysis-gas chromatography-mass spectrometry (py-GC/MS), which provides a molecular fingerprint after thermal, non-oxidative fragmentation and has been used to identify lignin, carbohydrate, lipid, aromatic and N-bearing fragments ([Stewart 2012](#)). This technique produces pyrolysis products that result in lignin monomers that are traced to lignin sources and are similar to the non-methylated compounds isolated using the more extensive cupric oxide extraction procedure and can detect relatively subtle changes in litter composition through decomposition. Fresh Litter and residues (FL, LR<sub>14d</sub>, LR<sub>6m</sub>, LR<sub>12m</sub>) biochemical composition was characterized by py-GC/MS at 550°C (Frontier pyrolyzer - Shimadzu QP-2010SE) with a SHRIIX-5ms column (30 m length x 0.25 mm ID, 0.25 µm film thickness). The initial column temperature was 40°C with a 1 min hold followed by a 7°C min<sup>-1</sup> ramp to 300°C and a final 5 min hold. The mass spectrometer detection range was 50–600 m/z with the interface temperature held at 300°C. Compounds were identified using the NIST 2011 mass spectral library and external standards including guaiacol, vanillin, vanillic acid, acetovanillone, syringol, syringaldehyde, acetosyringone, p-hydroxybenzoic acid, p-hydroxy acetophenone, p-hydroxybenzaldehyde, p-coumaric acid, and ferulic acid to verify pyrolysis products. Relative abundances are expressed as peak area as a proportion of identified peak area (%) with precision 2–7%. This expression of fragment composition is not quantitative, since samples were not externally calibrated.

## 2.4. Soil physical fractionation and chemical analyses of soil organic matter fractions

At the end of the second incubation all soils were analyzed to

determine the litter-derived C and N contribution to functionally distinct SOM fractions, and for their chemical diversity.

Soils were separated by size and density, into a dissolved organic matter (DOM), a light particulate organic matter (light POM; < 1.85 g cm<sup>-3</sup>), a heavy sand-sized OM (heavy POM; > 1.85 cm<sup>-3</sup> and >53 µm) and a mineral associated organic matter (MAOM >1.85 cm<sup>-3</sup> and <53 µm), as described in Mosier et al. (2021). We applied both size and density physical fractionation, to also separate the heavy sand-sized OM, which while typically represents a small fraction of SOM, it may behave differently from the light POM (Samson et al., 2020). Briefly, 6g of 2 mm oven-dried soil from each of the incubation units, was added to DI H<sub>2</sub>O, shook for 15 min, and then centrifuged at 1874 g for 15 min. The DOM fraction was poured off and analyzed for total organic C and total N on a Shimadzu TOC-L/TNM-L Analyzer (Shimadzu Corporation, Kyoto, Japan). In order to disperse aggregate structures, sodium polytungstate (1.85 g cm<sup>-3</sup>) and glass beads were added to the remaining soil in centrifuge tube, which were placed on a reciprocal shaker for 18 h. After dispersion, samples were centrifuged, and the light POM aspirated off the residual soil. This was thoroughly rinsed to remove any SPT and separated into heavy POM and MAOM by wet sieving at 53 µm. All fractions were analyzed for %C and %N, δ<sup>13</sup>C and δ<sup>15</sup>N on an EA-IRMS as described above. After fractionation, recoveries ranged from 96 to 104% for mass, from 65 to 106% with an average of 82% for C, and from 78 to 128% with an average of 97% for N.

To determine the effect of chemical diversity on soil organic matter formation, all bulk soils collected after the incubation were analyzed for their functional chemical groups using py-GC/MS as described above for the litter residues.

## 2.5. Microbial analyses of soils

To determine the effect of microbial community composition and diversity on soil organic matter formation, as affected by litter input structural and chemical diversity, DNA was extracted from all bulk soils collected after the incubation. DNA extractions were performed using a DNeasy PowerSoil 96-well plate DNA extraction kit (Qiagen, Hilden, Germany) following the standard protocol. DNA samples were quantified, amplified, and sequenced as described in (Albright et al., 2020) but modified to increase the number of PCR cycles in the first PCR to 25. Briefly, DNA samples were quantified with an Invitrogen Quant-iTTM ds DNA Assay Kit (Thermo Fisher Scientific, Eugene, OR, USA) on a BioTek Synergy HI Hybrid Reader (BioTek Instruments Inc., Winooski, VT, USA). PCR templates were prepared by diluting an aliquot of each DNA stock in sterile water to 1 ng/µL. The bacterial (and archaeal) 16S rRNA gene (V3–V4 region) was amplified using primers 515f-R806 (Bates et al., 2010). Henceforth, archaeal sequences were analyzed with bacterial sequences. The fungal 28S rRNA gene (D2 hypervariable region) was amplified using the LR22R primer (Mueller et al., 2016) and the reverse LR3 primer (Talbot et al., 2014). Preparation for Illumina high-throughput sequencing was undertaken using a two-step approach, similar to that performed by Mueller et al. (2015), with Phusion Hot Start II High Fidelity DNA polymerase (Thermo Fisher Scientific, Vilnius, Lithuania). In the first PCR, unique 6 bp barcodes were inserted into the forward and reverse primer in a combinatorial approach over 25 cycles with an annealing temperature of 60 °C (Gloor et al., 2010). The second PCR added Illumina-specific sequences over 10 cycles with an annealing temperature of 65 °C (Illumina, San Diego, CA, USA). Amplicons were cleaned using a Mo Bio UltraClean PCR clean-up kit (Carlsbad, CA, USA), quantified using the same procedure as for the extracted DNA, and then pooled at a concentration of 10 ng each. The pooled samples were further cleaned and concentrated using the Mo Bio UltraClean PCR clean-up kit. All clean ups were undertaken as per the manufacturer's instructions with the following modifications: binding buffer amount was reduced from 5X to 3X sample volume, and final elutions were performed in 50 µL Elution Buffer. A bioanalyzer was used to assess DNA quality, concentration was verified using qPCR, and paired-end 300 bp

reads were obtained using an Illumina MiSeq sequencer at Los Alamos National Laboratory. An internal control sample was included in the run to determine the fungal:bacterial ratio in each sample as described in detail previously (Hutchinson et al., 2021). All bacterial and fungal amplicon sequences were processed as described previously (Hutchinson et al., 2021).

## 2.6. Data and statistical analyses

The litter derived C (and N) contribution to CO<sub>2</sub> and each SOM fraction was calculated following Haddix et al. (2020). Briefly, we first determined the relative contribution ( $F_L$ ) of the labeled litter C (or N) to the CO<sub>2</sub> or SOM fraction using a two-end member mixing model (Eq. (1)) (Boutton, 1996) and then we multiplied the  $F_L$  value by the amount of C (or N) in the same pool, by replicate sample.

$$F_L = \frac{\text{atom}\%^{13}\text{C}_m - \text{atom}\%^{13}\text{C}_C}{\text{atom}\%^{13}\text{C}_L - \text{atom}\%^{13}\text{C}_C} \quad (1)$$

In Eq. (1),  $F_L$  is the fraction of labeled litter-derived C for each replicate, atom%<sup>13</sup>C<sub>m</sub> is the atom percent<sup>13</sup>C in the pool of interest for each litter treatment sample, atom%<sup>13</sup>C<sub>C</sub> is the average percent<sup>13</sup>C in the corresponding control pool, and atom%<sup>13</sup>C<sub>L</sub> is the average percent<sup>13</sup>C of the C in the initial labeled litter. We report litter derived C and N recoveries in percent of the litter C and N added, because those varied slightly by litter input type (Table 1).

A one-way ANOVA was run by litter type for the five litters (LL, FL, LR<sub>14d</sub>, LR<sub>6m</sub>, LR<sub>12m</sub>) for C:N, <sup>13</sup>C and <sup>15</sup>N and for the four litters (FL, LR<sub>14d</sub>, LR<sub>6m</sub>, LR<sub>12m</sub>) for %C, %N, HWE, NHF, AHF, AUF, LCI using the car package in R (Fox and Weisberg 2019). A two-way ANOVA was run by litter type (LL, FL, LR<sub>14d</sub>, LR<sub>6m</sub>, LR<sub>12m</sub>) and soil depth (0–10 cm and 120–150 cm) for litter stabilized in whole soil and soil fractions, undecomposed litter, respired litter, and stabilization efficiency using the car package in R (Fox and Weisberg, 2019). A two-way ANOVA with repeat measures was used for soil respiration rates with sample as a random effect using the lmer function in the lmerTest package in R. Multiple comparisons of treatments by the least significant difference were used to determine differences for litter chemistry by litter type and cumulative CO<sub>2</sub> respiration, and litter C and N recovered in SOM and SOM fractions by litter type for each soil at the end of the experiment using the LSD test in the agricolae package in R.

The chemical diversity of the litter obtained from the first incubation and soil residues from the second incubation were determined using the 'vegan' package (v. 2.5–6) diversity function on the relative abundance data obtained from py-GC/MS analyses. The litter py-GC/MS relative abundance biomarker data were analyzed using distance-based redundancy analysis (dbRDA). Bray's distance was used to examine chemical differences between litter chemistry. Eigenvalues obtained from a principal coordinate analysis (PCoA) on the distance matrix were used for a redundancy analysis. Permutation-based analysis of variance (ANOVA) was performed on all dbRDA models to determine significance among group differences. Ellipsoids represent 95% confidence intervals around the multivariate-group centroids.

All microbial composition, diversity, and abundance analyses were conducted in R version 3.6.0 (R Core Group, 2019). Sequences were analyzed using phyloseq (McMurdie and Holmes, 2013) where samples were rarefied to 2500 for both bacteria and fungi. This rarefaction resulted in four samples (Topsoil\_NL\_2, Topsoil\_LL\_1, Subsoil\_LL\_4, Topsoil\_LR<sub>14d</sub>\_1) not proceeding for further analysis. As a proxy of microbial community composition often linked to litter decomposition rates and SOM formation efficiencies (Ekschmitt et al., 2008), we also quantified fungal:bacterial (F/B) ratios. To determine F/B ratios, samples were processed as described in Hutchinson et al. (2021) using an internal control. Briefly, after rarefaction to the same depth for bacterial and fungal sequences, the counts of the internal control from the bacterial OTU table were divided by the counts of the internal control in the

**Table 1**

Litter chemistry at the different harvests. C and N concentration are in percent for fresh litter (FL) and litter residues (LR) and mg/L for litter leachates (LL). Subscripts indicate the days (d) or months (m) leachates and residues were collected from the start of the first decomposition experiment. Hot Water Extract (HWE), neutral hydrolyzable fraction (NHF), acid hydrolyzable fraction (AHF) and acid-unhydrolyzable residue (AUF) are reported in % mass. Because of the extraction procedure NHF also contain HWE. LCI is the lignocellulose index [AHF/(AUF + AHF)]. Data are means  $\pm$  1 sem, n = 4. P values are from one-way ANOVA by litter type. Letters denote differences at p < 0.05 by litter type.

Treatment	C (% or mg/L)	N (% or mg/L)	C:N	$^{13}\text{C}$ atom %	$^{15}\text{N}$ atom %	HWE %	LCI
FL	43.53 $\pm$ 0.14a	0.97 $\pm$ 0.05b	45.35 $\pm$ 2.15a	4.61 $\pm$ 0.01 ab	6.63 $\pm$ 0.04a	22.23 $\pm$ 0.65a	0.12 $\pm$ 0.01a
LL <sub>14d</sub>	2.77 $\pm$ 0.32a	0.17 $\pm$ 0.02	16.75 $\pm$ 0.63c	4.38 $\pm$ 0.03c	6.10 $\pm$ 0.07b		
LR <sub>14d</sub>	43.72 $\pm$ 0.52a	1.00 $\pm$ 0.06b	44.15 $\pm$ 2.92a	4.63 $\pm$ 0.02a	6.69 $\pm$ 0.02a	17.53 $\pm$ 0.82b	0.16 $\pm$ 0.00b
LR <sub>6M</sub>	43.31 $\pm$ 0.54a	1.38 $\pm$ 0.03a	31.44 $\pm$ 0.64b	4.57 $\pm$ 0.01 ab	6.70 $\pm$ 0.01a	8.61 $\pm$ 0.68c	0.27 $\pm$ 0.00a
LR <sub>12M</sub>	43.18 $\pm$ 0.06a	1.46 $\pm$ 0.05a	29.71 $\pm$ 1.10b	4.55 $\pm$ 0.01b	6.69 $\pm$ 0.02a	7.29 $\pm$ 0.41c	0.30 $\pm$ 0.01a
P value	0.765	<0.001	<0.001	<0.001	<0.001	<0.001	<0.001

fungal OTU table to produce a F/B ratio. Then, an aggregated OTU table was created by scaling the fungal OTU counts relative to bacterial OTU counts using the F/B ratio. The internal control was removed from all OTU tables prior to further analysis. Using the aggregated OTU table, diversity analyses were conducted in phyloseq using the “diversity” function. Topsoil and subsoil samples were separated prior to computing a Bray-Curtis dissimilarity matrix using the “ordinate” function due to high dispersion. PERMANOVA of treatment effect on surface and sub-surface soils was determined using the “adonis” function.

The relationship between chemical diversity, microbial diversity, F/B ratios, chemical-physical analyses of litter, and stabilization efficiencies of litter-derived C in SOM, POM, and MAOM were analyzed using the linear regression Pearson's product moment correlation coefficient functions in the stats package (v. 3.6.0). All plots were made using the packages ggplot2 (v. 3.3.2), ggpublisher (v. 0.4.0) and ggmisc (v. 0.3.7).

### 3. Results

#### 3.1. Litter mass loss and chemical changes during the first incubation

During the first incubation, litter mass loss in percent of initial was on average 22% after 14 days, 54% after six months, and 60% after 12 months of incubation. Litter mass loss was distributed between  $\text{CO}_2$  and DOM leaching in different proportions over time (Fig. 1). Litter residues composition changed during decomposition, with a significant

reduction over time in the concentration of the NHF (p < 0.001), a lack of change in the concentration of AHF (p = 0.74) and a significant relative accumulation of AUF (p < 0.001; Fig. 1).

Bulk litter C concentration remained the same (43%) from fresh litter to litter residues over time, but %N increased, resulting in progressively decreasing C:N of litter residues during decomposition (Table 1). Litter leachates collected during the first 14 days of incubation, had much lower %C and higher %N, than any of the litter residue, resulting in LL<sub>14d</sub> being the litter input type with the lowest C:N (Table 1). The fraction of HWE in litter residues decreased over time of decomposition, with fresh litter having the most and LR<sub>12M</sub> having the least, while the LCI significantly increased over time, as the AUF relatively accumulated in the litter residue (Fig. 1, Table 1). All litter types were highly enriched in  $^{13}\text{C}$  (>4 atom%) and  $^{15}\text{N}$  (>6 atom%; Table 1), enabling accurate tracing in the following incubation.

Fresh litter was chemically distinct from the more decomposed litters and clustered separately from the litter residues for chemical composition as determined by Py-GC/MS (p < 0.001, Fig. 2). The first axis explained 75% of the variation with separations between carbohydrate-derived (2,5-Furandione, 3-methyl) and lignin-derived (4-vinylphenol) biomarkers between the fresh and litter residue. The second axis explained 15% of variability between samples and predominantly separated the LR<sub>14d</sub> samples along guaiacol lignin biomarker. Only structural litter types were used for these analyses, and the initial chemical diversity of LL was not assessed.

#### 3.2. Carbon and nitrogen dynamics during the litter residues and leachates incubation in soils

At the beginning of the incubation all litters started with relatively high respiration rates (Fig. 3 a, b inserts), with rates differing among litter types (p < 0.0001) in the order LL > FL > LR<sub>14d</sub> >> LR<sub>6M</sub> = LR<sub>12M</sub>, with the latter two having very low respiration rates, as expected. It is worth notice, that the FL respiration less than LL, indicating that HWE are less accessible to microbial breakdown when present within plant tissues than if added to the soil as leachates. Both litter and soil interacted significantly with time (p < 0.0001), and the three-way interaction was also significant (p < 0.0001). For all litter inputs respiration declined quickly already within the first 14 days (Fig. 3 a, b inserts) and reached an asymptote after around 112 days for the topsoil and 70 days for the subsoil, after which all litters came together, and maintained relatively low  $\text{CO}_2$  loss rates till the end of the incubation. Litter respiration dynamics were similar between the two soils, but rates differed (p < 0.0001) and were much higher in the topsoil (Fig. 3a and b), resulting in lower cumulative  $\text{CO}_2$  losses in the subsoil (Fig. 3c). Litter types behaved similarly in both soils (p = 0.06), with the FL and the LL having higher cumulative  $\text{CO}_2$  losses than the three LR litter types (Fig. 3c).

By the end of this one-year incubation in soil, litter C and N recoveries varied in the range 57–76% and 46–81%, respectively (Fig. 4). For C, the majority of the litter C recovered was in the  $\text{CO}_2$  (on average 37%) with significantly higher  $\text{CO}_2$  losses in the topsoil (p < 0.001) and

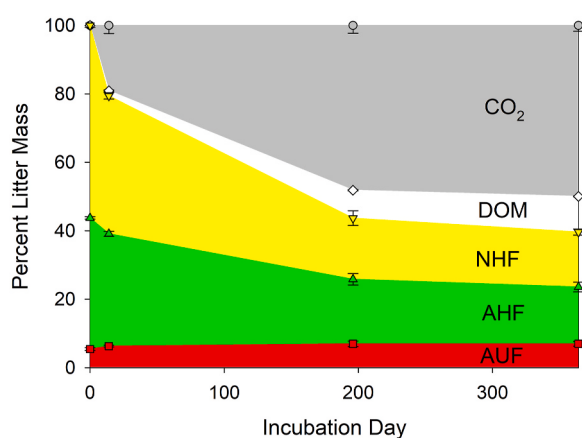


**Fig. 1.** Mass loss in percent of the initial litter mass to carbon dioxide ( $\text{CO}_2$ ) and dissolved organic matter (DOM), and percent change in the litter residue remaining component fractions, during one year of incubation of Sorghum bicolor leaves. Litter residues component fractions were analyzed by wet chemistry as a neutral hydrolysable fraction (NHF, proxy for hemicellulose), an acid hydrolysable fraction (AHF, proxy for cellulose), and an acid unhydrolysable fraction (AUF, proxy for lignin and other chemically recalcitrant litter and microbial compounds). Symbols are means, with standard errors as bar (n = 4).

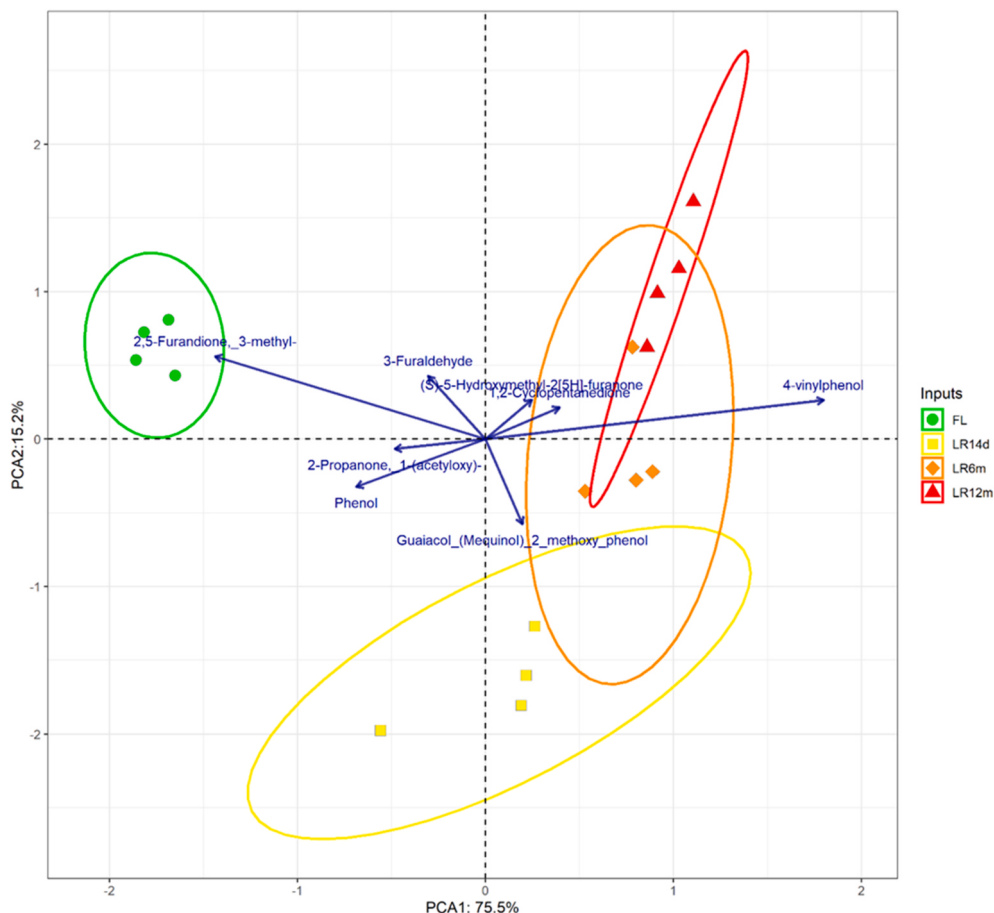


**Fig. 2.** Principle component analysis of biomarker chemical data from py-GC/MS in the four structural Sorghum litter input types [fresh litter (FL), litter residues collected after 14 day (LR<sub>14d</sub>), 6 months (LR<sub>6m</sub>) and 12 months (LR<sub>12m</sub>) of decomposition].

for the FL and LL types ( $p < 0.001$ ). Consistently more C remained in the undecomposed residue in the subsoil of the LRs, with a significant litter x soil interaction ( $p < 0.01$ ; Fig. 4a). The litter derived-C recovered in soil was higher for the LL and LRs than for FL ( $p < 0.001$ ), but not significantly different between the subsoil and the topsoil ( $p = 0.341$ ; Fig. 4a). For N, there was more N recovered in soil from the LL than from any other litter types and across all treatments more litter-derived N remained in the subsoil than the topsoil ( $p = 0.004$ ; Fig. 4b). Both litter and soil types had significant effects on N recovered in residue ( $p < 0.001$ ) as well as a significant interaction ( $p < 0.001$ ), with more N recovered in residues from the LRs than from FL, and in the subsoil than topsoil (Fig. 4b).

The distribution of litter derived C and N among SOM fractions varied significantly across litter types ( $p < 0.001$  for both C and N), with the LL contributing most to MAOM, and the highly decomposed residues (LR<sub>6m</sub> and LR<sub>12m</sub>) contributing most to light POM (IPOM) as hypothesized, both for C and N (Fig. 5). This behavior was even more pronounced for the subsoil than for the topsoil, with differences between soils being significant for DOM and heavy POM (hPOM) for C ( $p < 0.001$ ), and for all fractions for N (IPOM  $p < 0.02$ ; all others  $p < 0.001$ ; Fig. 5). Both litter-derived C and N contributed negligible amounts to hPOM, therefore we focus our discussion below on the IPOM, which we refer to for simplicity as POM. Small litter derived C amounts were recovered in DOM (Fig. 5a), while a relatively high percentage of litter derived N was recovered in soil solution (DOM) for the topsoil and the LL treatment (Fig. 5b). Only occasionally litter versus soil interactions were significant, for litter-derived C in DOM and IPOM ( $p < 0.05$ ) and for litter-derived N in IPOM ( $p < 0.01$ ).

### 3.3. Soil chemical and microbial diversity

After incubation soils strongly separated for their chemical composition, as measured by py-GC/MS, between topsoils and subsoils (Fig. 6). The latter remained chemically similar across the different litter input types, while topsoils spread more broadly, despite this, they did not clearly cluster by litter input type. Axis 1 separated along aromatic phenol in the topsoil and benzonitrile in the subsoil.

By the end of the incubation, microbial community was different between the two soils, and was in many ways affected by the different litter input types. Microbial biomass, as determined by DNA concentration, was significantly higher in the topsoil (Tukey HSD  $p$  adj = 0) compared to subsoil, but there was no effect of litter input type on microbial biomass ( $p$  adj.  $> 0.05$ ). Overall, addition of FL and LRs increased microbial biomass in both soils, but not the LL addition, or LR<sub>12m</sub> in the topsoil (Fig. S1). Similarly, microbial community composition was significantly different between the two soils (Adonis  $R^2 = 0.50$ ,  $p = 0.001$ ) and affected by the litter inputs (Adonis topsoil  $R^2 = 0.69$ ,  $p = 0.001$ , subsoil  $R^2 = 0.52$   $p = 0.001$ ) as measured by Bray-Curtis dissimilarity (Fig. S2). The dispersion was significantly different between the two soils (ANOVA  $F = 153.99$ ,  $p = 1.23e-15$ ), but was not significantly different between litter type within each soil (Topsoil: ANOVA  $F = 4.02$ ,  $p = 0.16$ , Subsoil: ANOVA  $F = 0.40$ ,  $p = 0.84$ ). Consistently, F/B ratios were highest in the FL compared to other litter input types for both the topsoil and subsoil. Overall, soil type did not affect F/B ratio, while litter input type did significantly alter the F/B ratio in both soil types ( $p = 0.01$ ; Fig. S4).

Microbial diversity did not significantly differ between the two soils but was significantly different between litter types (ANOVA  $F = 13.10$ ,

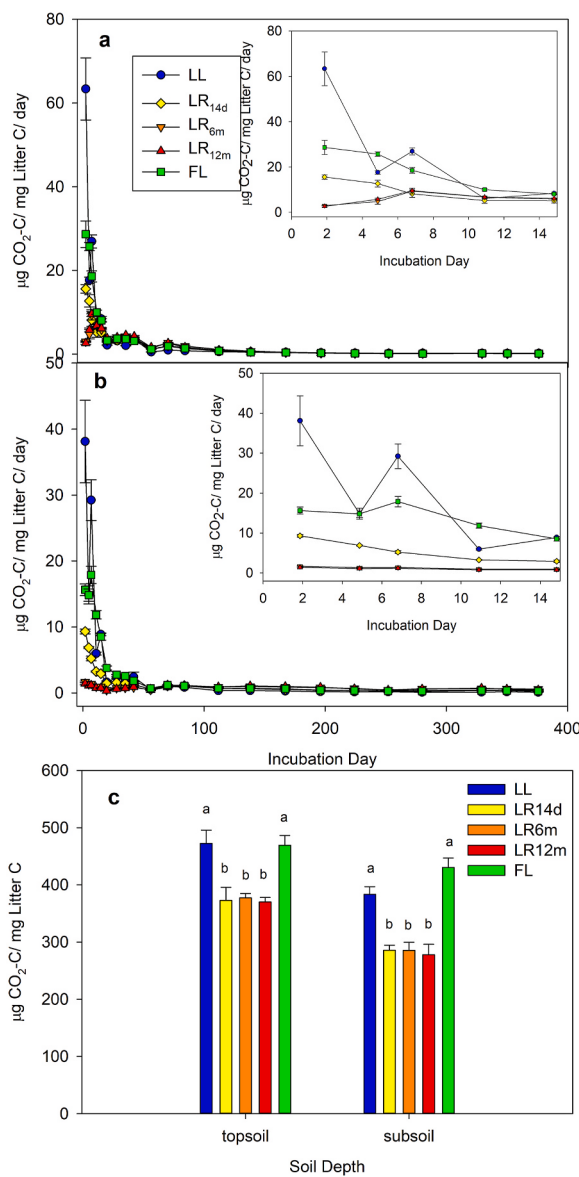


**Fig. 3.** Litter respiration rates for Sorghum fresh litter (FL), the litter leachates (LL), and the litter residues collected after 14 day (LR<sub>14d</sub>), 6 months (LR<sub>6m</sub>) and 12 months (LR<sub>12m</sub>) of decomposition, and incubated in topsoil (a), and subsoil (b); and cumulative CO<sub>2</sub> respired after the one-year incubation for all litter types in the two soils (c). Letters in panel c denote differences at  $p < 0.05$  within soil comparisons by litter. Symbols are means, with standard errors as bar ( $n = 4$ ).

$p = 4.7e-06$  and their interaction (ANOVA  $F = 3.61$ ,  $p = 0.018$ ) (Fig. 7). In the topsoil, the addition of FL and LRs increased the soil microbial diversity, with the highest diversity observed for LR<sub>14m</sub>, while the addition of LL did not modify the soil microbial diversity. Responses were lower for the subsoil, where only the addition of LRs types increased the soil microbial diversity (Fig. 7).

To explain drivers of microbial diversity we evaluated the effect of litter input properties (i.e., %HWE, %LCI) on microbial diversity by linear regression. In the topsoil, LCI was negatively related to microbial diversity ( $R^2 = 0.317$ ,  $p = 0.029$ ) while HWE had a significant negative relationship with microbial diversity in the subsoil ( $R^2 = 0.252$ ,  $p = 0.048$ ; Supplemental Fig. 3). There was no significant relationship between microbial and chemical diversity for either the topsoil or the subsoil (Fig. S5). Furthermore, there was no significant relationship between litter input properties and chemical diversity except for HWE in

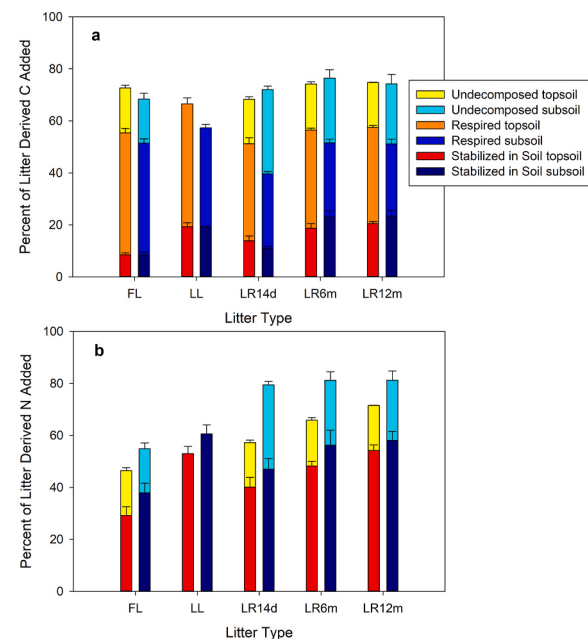


**Fig. 4.** Litter derived carbon (a) and nitrogen (b) for the five Sorghum litter input types [fresh litter (FL), litter leachates (LL), and litter residues collected after 14 day (LR<sub>14d</sub>), 6 months (LR<sub>6m</sub>) and 12 months (LR<sub>12m</sub>) of decomposition] recovered as CO<sub>2</sub> (for carbon), remaining residue, or bulk soil after one year of incubation in topsoil or subsoil. P values are two-way ANOVA by litter type and soil depth.

the subsoil, which had a negative relationship with chemical diversity ( $R^2 = 0.39$ ,  $p = 0.032$ ; Fig. S6).

#### 3.4. Efficiencies and drivers of litter derived IPOM and MAOM formation

The efficiency of stabilization of litter-derived C in IPOM and MAOM varied between less than 1% and 14%, and differed significantly between litter input types ( $p < 0.001$  for both IPOM and MAOM) and soils (IPOM: $p = 0.036$ , MAOM: $p = 0.047$ ). Given the small amount of input-derived C in hPOM we did not investigate its stabilization efficiency. The soluble input (LL) had the highest MAOM stabilization efficiency, while the more decomposed LR had the highest IPOM efficiency (Fig. 8). In general stabilization efficiencies were higher in the subsoil than the topsoil, with a significant litter  $\times$  soil interaction for the POM stabilization ( $p < 0.01$ ; Fig. 8a).

Both chemical and microbial diversity were positively and linearly related to the stabilization efficiency of POM, with the regression being significant for both in the subsoil, and for microbial diversity in the topsoil as well (Fig. 9). Efficiency of litter-derived C stabilization in POM was not related to soil F:B ratio (Fig. S7). By contrast, the stabilization efficiency in MAOM was only significantly related to microbial diversity in the topsoil with a negative linear relationship (Fig. 10), and across soils it was also negatively related to the soil F:B ratio (Fig. S7). Removing the litter leachate input from the analyses of MAOM formation, the subsoil chemical diversity became significant (Fig. 10D;  $R^2 = 0.454$ ,  $p = 0.004$ ).

#### 4. Discussion

We performed a two-tiered laboratory incubation to investigate the effect of plant input physical-chemical properties, through the addition of soluble *versus* structural residues at differing stages of decomposition, on (1) the pathways of SOM formation (2) the soil microbial community and chemical diversity, and (3) their interaction on the stabilization efficiency of litter-derived C in POM and MAOM, in a topsoil and a

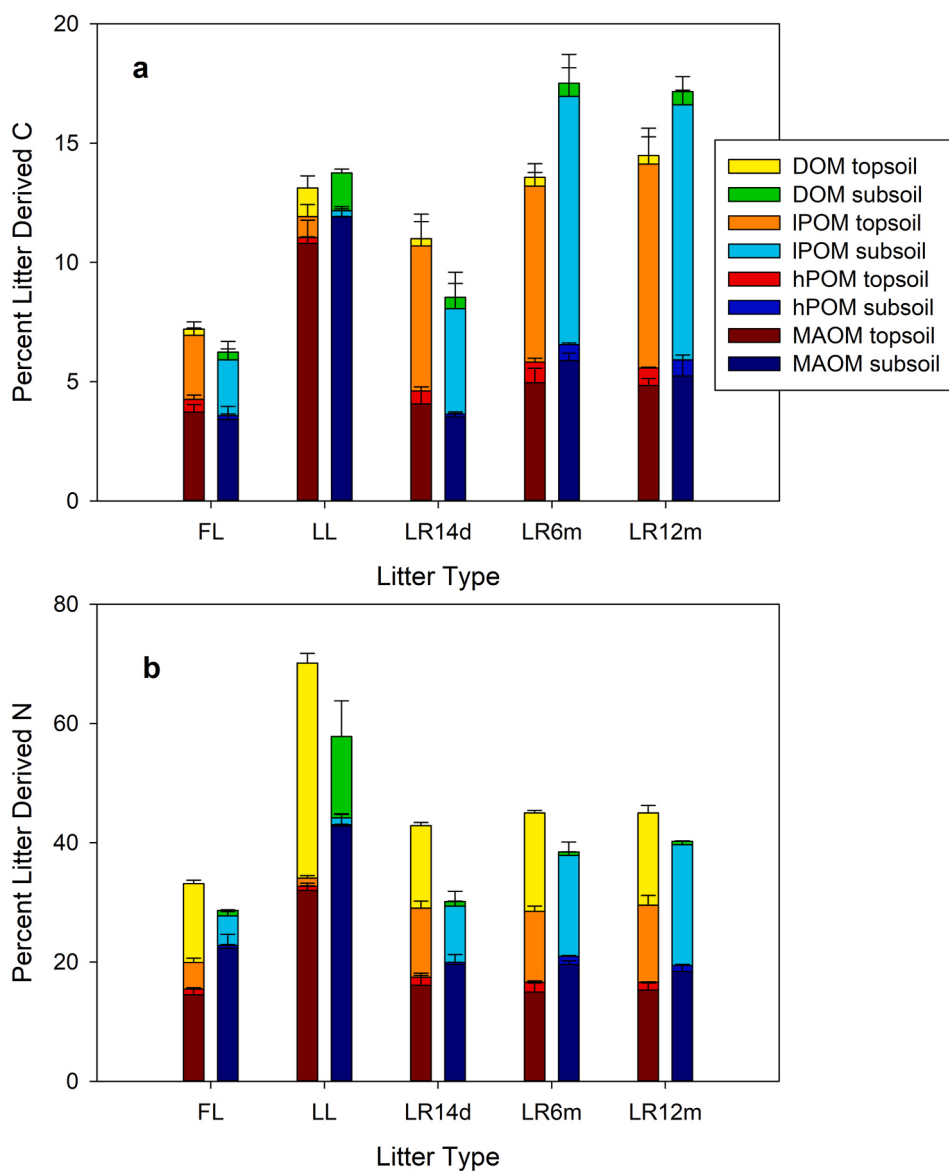


**Fig. 5.** Litter derived carbon (a) and nitrogen (b) for the five Sorghum litter input types [fresh litter (FL), litter leachates (LL), and litter residues collected after 14 day (LR<sub>14d</sub>), 6 months (LR<sub>6m</sub>) and 12 months (LR<sub>12m</sub>) of decomposition] recovered in soil solution/as dissolved organic matter (DOM); light particulate organic matter (IPOM), heavy particulate organic matter (hPOM), and mineral associated organic matter (MAOM), after one year of incubation in topsoil or subsoil.

subsoil. Overall results demonstrated that: i) the most important driver of both the pathways and efficiencies of SOM formation is the physical nature of the plant input, since the biggest differences were observed between soluble *versus* structural plant inputs; ii) for structural residues the relative efficiency of POM formation increases with time from decomposition, linearly with an increase of microbial and chemical diversity in soil, the latter only for subsoil; ii) more input-derived C and N are retained in subsoil as a result of both higher stabilization in MAOM and slower residue decay. Our results also confirm the importance of direct sorption of soluble inputs to silt and clay sized minerals for the formation of MAOM in bulk soils (Sokol et al., 2019). In fact, we observed the highest efficiency of MAOM formation from soluble inputs (LL) without a parallel increase in either microbial biomass or diversity, suggesting that most of the MAOM formation was performed abiotically by direct sorption (Sanderman et al., 2014). The high efficiency of microbial transformation of the LL may have also contributed to the high efficiency of MAOM formation from LL.

#### 4.1. Residue decomposition and pathways of SOM formation

To understand the pathways of SOM formation from plant inputs differing for their physical properties (i.e., soluble *versus* structural) and chemical composition, we preincubated dual labeled (<sup>13</sup>C and <sup>15</sup>N) sorghum fresh litter for a year, and obtained five types of input with differing proportion of soluble (or HWE) material, from 100% (LL) to 7.2–8% (FL-LR<sub>6m</sub>; Table 1), and significantly different chemical composition as characterized by fiber analyses (Fig. 1) and by Py-MS (Fig. 2).

We traced these residues C and N in CO<sub>2</sub>, and in the soil as undecomposed residues, and SOM fractions, however we did not obtain a full recovery, possibly due to volatile losses other than CO<sub>2</sub>, including VOC (Gray et al., 2010) and N gases (Davidson and Swank 1986) for C and N, respectively. Fresh and DOM inputs (FL and LL) lost relatively more of their C as CO<sub>2</sub> than the structural residues, even if with different dynamics (Fig. 3), as expected given they had not undergone previous microbial transformation. Surprisingly the LR<sub>14d</sub> lost the same relative amount of C to CO<sub>2</sub> as the more decomposed LR (Fig. 3c), despite it had

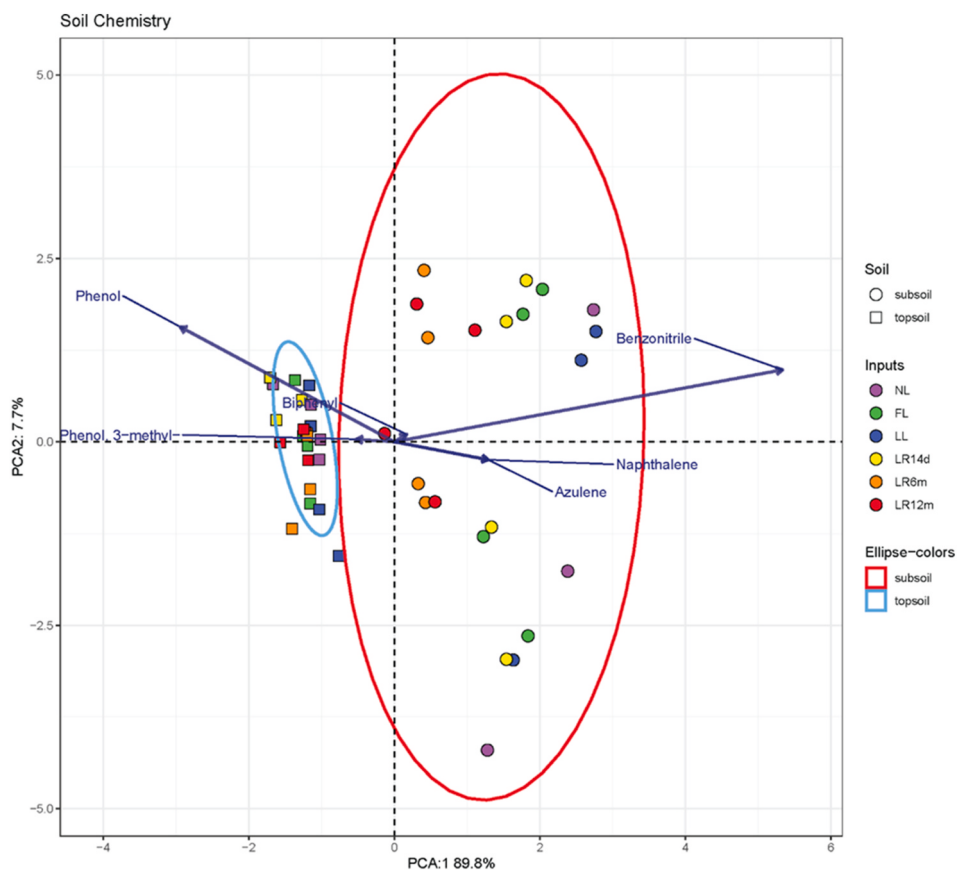


**Fig. 6.** Final soil chemical composition (py-GC/MS) for the topsoil and subsoil incubated for one year with no-litter (NL) or with five Sorghum litter input types [fresh litter (FL), litter leachates (LL), and litter residues collected after 14 day (LR<sub>14d</sub>), 6 months (LR<sub>6m</sub>) and 12 months (LR<sub>12m</sub>) of decomposition].

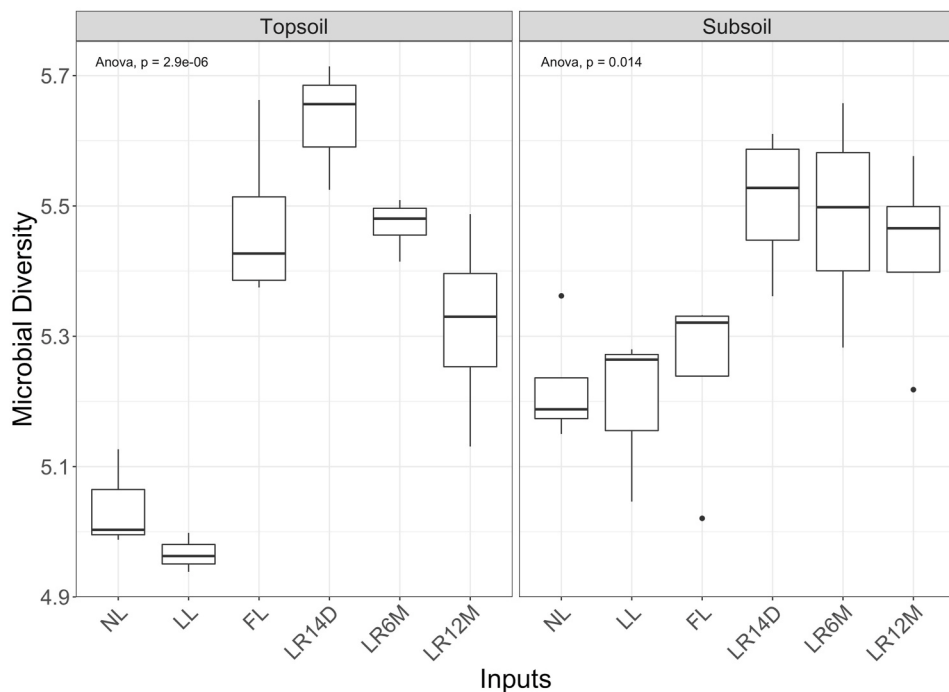


**Fig. 7.** Shannon diversity of the microbial community in the topsoil and subsoil after one year of incubation with the five Sorghum litter input types [fresh litter (FL), litter leachates (LL), and litter residues collected after 14 day (LR<sub>14d</sub>), 6 months (LR<sub>6m</sub>) and 12 months (LR<sub>12m</sub>) of decomposition], or without any input (NL). Global ANOVA p-value is reported using `stat_compare_means` function.

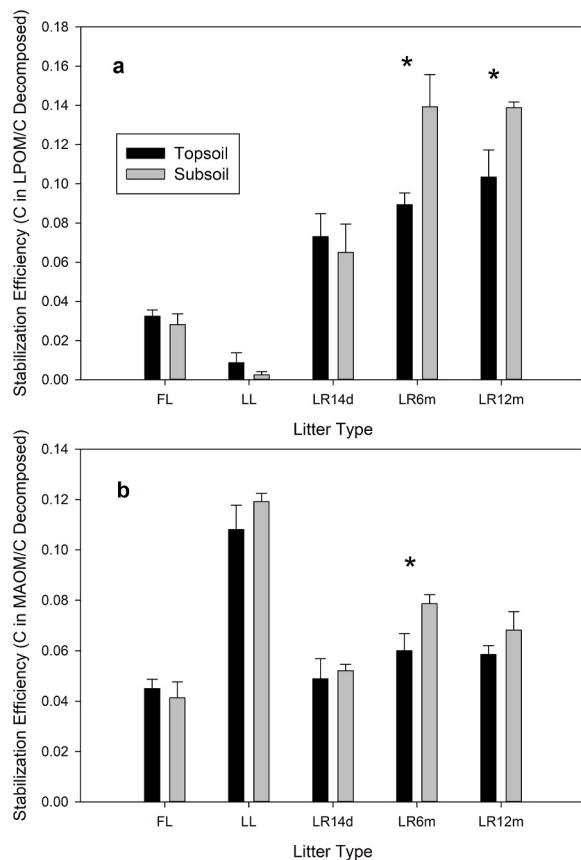


**Fig. 8.** Stabilization efficiency of litter-derived C in IPOM (a) and MAOM (b) for the five Sorghum litter input types [fresh litter (FL), litter leachates (LL), and litter residues collected after 14 day (LR<sub>14d</sub>), 6 months (LR<sub>6m</sub>) and 12 months (LR<sub>12m</sub>) of decomposition] after one year of incubation in topsoil (0–10 cm) or subsoil (120–150 cm). Asterix denote significant differences between soils ( $p < 0.05$ ).

undergone less mineralization during the first incubation (Fig. 1). The LR<sub>14d</sub> separated from the other LRs for its chemical makeup particularly driven by a higher abundance of guaiacol lignin biomarker (Fig. 2). This chemical makeup must have rendered the LR<sub>14d</sub> higher stability, particularly in the subsoil, where a higher proportion of it accumulated as undecomposed residue as compared to other structural residues (Fig. 4). While more work relating specific fiber chemistries to their decomposability on the litter layer *versus* incorporated within top and subsoil is required, our results point to relatively high residue stability, for structural residues deprived of the initial leachates when incorporated in the soil, and particularly in the subsoil. These findings are consistent with other studies observing decreased mineralization of grass residues incorporated within the bulk soil (Mitchell et al. 2016, 2018; Leichty et al., 2020), and suggests that incorporation of leached residues in the subsoil can be an effective means to decrease residue C losses to CO<sub>2</sub>. Overall, the amount of litter-derived C remaining in the soil in this study was lower than what we found in a field incubation of the fresh residue of the same Sorghum litter, where 19% of the initial litter C was recovered in the soil after 19 months of incubation (Fulton-Smith and Cotrufo 2019). Likely the fact that in this study litter was cut to 1 cm might have increased the relative C losses through mineralization. Taken together, this study suggests that the optimal plant residue management for soil C sequestration is through leaching and subsequent incorporation of the intact structural residue into the subsoil.

Confirming our hypothesis and consistently with the two pathways model of SOM formation (Cotrufo et al., 2015), soluble plant inputs (LL) resulted in the highest relative amount of input-derived C and N remaining in MAOM (Fig. 5). Other studies have observed fast and efficient SOM or more specifically MAOM formation following the input of soluble compounds or plant-derived DOM (Strickland et al., 2012; Kallenbach et al., 2016; Lynch et al., 2018). However, water solubility does not necessarily appear as the exclusive property driving efficient MAOM formation. When comparing the effects of animal manure addition to MAOM formation, Samson et al. (2020) observed equally high MAOM formation from the addition to soil of solid poultry and liquid dairy manures, but lower MAOM formation from the addition of liquid swine manure. The very high nutrient content of animal manure

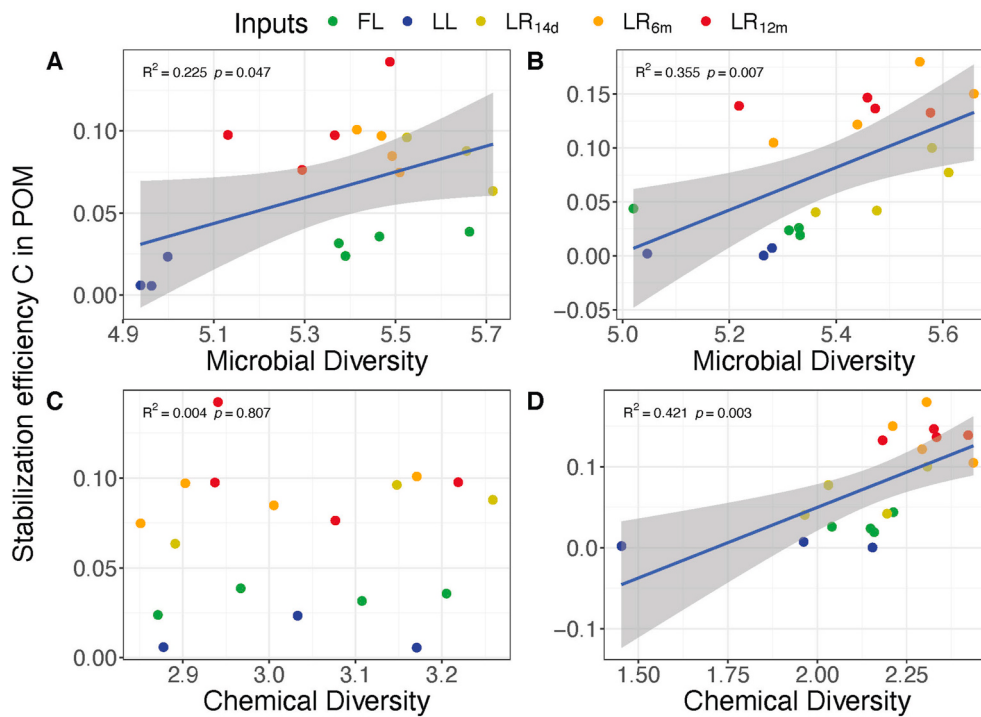


**Fig. 9.** Relationship between the stabilization efficiency of litter-derived C in POM and microbial Shannon diversity of the (A) topsoil and (B) subsoil or chemical Shannon diversity of the (C) topsoil or (D) subsoil, after one year of incubation with five Sorghum litter input types [fresh litter (FL), litter leachates (LL), and litter residues collected after 14 day (LR<sub>14d</sub>), 6 months (LR<sub>6m</sub>) and 12 months (LR<sub>12m</sub>) of decomposition]. R<sup>2</sup> and p-values from linear regression within each soil depth are reported.

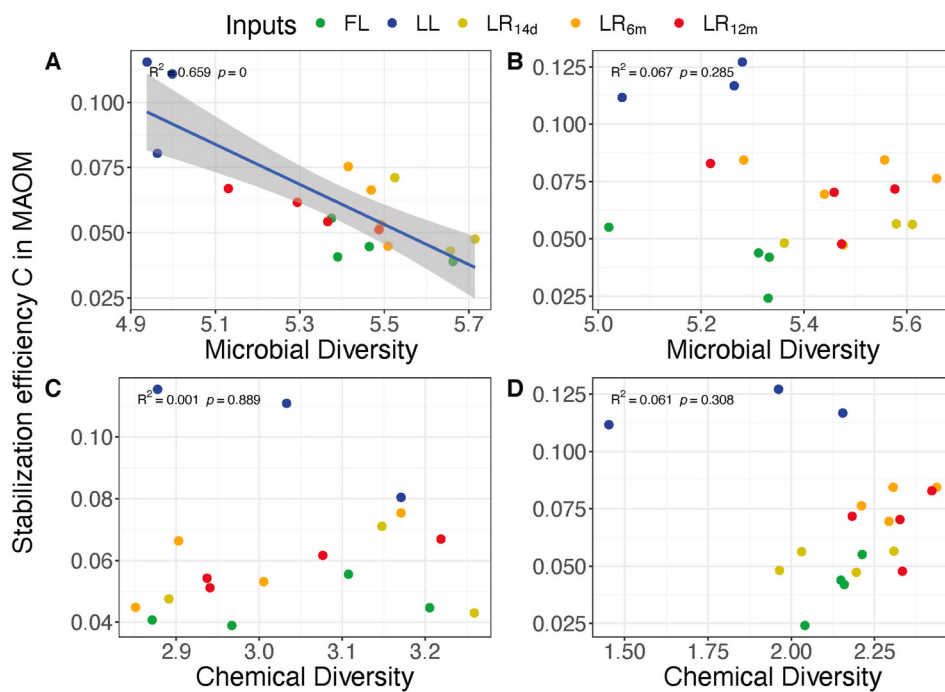


**Fig. 10.** Relationship between the stabilization efficiency of litter-derived C in MAOM and microbial Shannon diversity of the (A) topsoil and (B) subsoil or chemical Shannon diversity of the (C) topsoil or (D) subsoil, after one year of incubation with five Sorghum litter input types [fresh litter (FL), litter leachates (LL), and litter residues collected after 14 day (LR<sub>14d</sub>), 6 months (LR<sub>6m</sub>) and 12 months (LR<sub>12m</sub>) of decomposition].  $R^2$  and p-values from linear regression within each soil depth are reported.

may drive different dynamics of SOM formation and priming, making them hard to compare to the dynamics observed after the addition of plant inputs. In our study, the addition of plant residues also resulted in MAOM formation, despite its lower relative proportions when compared to LL additions (Fig. 5). All our residues had a significant amount of water soluble and hydrolysable fibers (Fig. 1, Table 1), and we expect that MAOM was formed from both the microbial *ex-vivo* and *in-vivo* transformation of these inputs and the subsequent association to minerals of the produced DOM and microbial residues (Liang et al., 2017).

Following our expectation, the more decomposed structural residues (LR<sub>6m</sub> and LR<sub>12m</sub>) resulted in the highest relative amount of POM formation, specifically in the light POM fraction. Light POM has been consistently observed to have similar characteristics to plant residues (Christensen 2001), and has long been considered to be the direct product of plant litter decomposition (Grandy and Neff 2008). However, the decomposition and microbial transformation of POM is also expected to be the precursor for MAOM formation (Grandy and Neff 2008; Lehmann and Kleber 2015). While we did not follow POM turnover over time, there was no indication of lower POM accumulation (e.g., in the FL) resulting in more MAOM formation (Fig. 5). On the contrary, some IPOM was formed in the topsoil from the addition of LL, indicating the contribution of microbial structural components to this pool. Overall, this study further supports our previous findings of independent formation pathways of POM and MAOM from different components of plant inputs (Cotrufo et al., 2015; Haddix et al. 2016, 2020), stressing the need to represent these independent formation pathways in models (Zhang et al., 2021).

#### 4.2. Effects of residue inputs on soil chemical and microbial diversity

Upon incubation of significantly different plant inputs for physical structure, degree of decomposition, and chemical composition (Figs. 1 and 2), we did not observe a modification in the chemical composition of soils, which remained distinct between topsoil and subsoil (Fig. 6). In our incubation, litter inputs represented 3%–0.07% of the native soil C to the subsoil, respectively for LRs and LL, and 0.07%–0.01% C of the native soil C to the topsoil, respectively for LRs and LL. These amounts are within the range of expected plant C inputs to soils [calculated using inputs for grasslands from (Cotrufo and Lavallee 2021) and stocks from

(Lugato et al., 2021)], indicating that while soil chemistry typically reflects long term plant inputs (Collins et al., 2000), it will not be quickly modified by fresh annual inputs. Consistently, but contrary to our hypothesis the chemical diversity of our plant inputs did not significantly correlate to the soil microbial diversity ( $R^2 = 0.032, p = 0.84$ ; Fig. S5). The latter however was significantly different across the different inputs, both in the topsoil and subsoil (Fig. 7), indicating that the physical structure and degree of decomposition of the inputs are larger drivers of microbial diversity than its chemical diversity. Interestingly the different inputs modified soil microbial diversity with different patterns across the two soils. In the subsoil, microbial diversity was increased by the more decomposed inputs (LRs) and all by a similar amount, whereas in the topsoil only the LL did not affect microbial diversity which was increased by all the other inputs in different amounts (Fig. 7). As litter decompose, microbial communities develop within the litter residues (Bani et al., 2018), thus the residue addition to soil enrich the soil community of new and diverse microbes.

Fungal to bacteria (F:B) ratio has long been considered a driver of soil carbon dynamics (Six et al., 2006), with lower residue mineralization and more efficient SOM formation in soils with fungal dominated microbial communities (Malik et al., 2016). Our soil microbial communities were overall dominated by bacteria, and the addition of litter residues slightly increased the fungal abundance (Fig. S4). This resulted in a negative correlation between F:B and MAOM formation, which most likely was an indirect effect of the highest litter-derived C stabilization efficiency in MAOM from soluble inputs in soils with low fungal abundance (Fig. S6).

#### 4.3. Efficiencies and drivers of POM and MAOM formation from plant inputs

After one year of incubation, stabilization efficiencies varied between 1 and 15%, and 4–12% respectively for POM and MAOM, which are at the low end of the range of previously reported SOM stabilization efficiencies (Castellano et al., 2015). As we hypothesized, both litter input and soil type significantly affected litter-derived stabilization efficiencies in both POM and MAOM, with the highest values observed in the subsoil for POM from the more decomposed structural residues (LR<sub>6m</sub> and LR<sub>12m</sub>) and for MAOM from the soluble inputs (LL). As

mentioned above, these results fully support the two pathways model of SOM formation (Cotrufo et al., 2015), as well as the expectation that plant input to subsoils will result in the most efficient C sequestration due to both lower C saturation and therefore capacity for MAOM formation, but also lower decomposition rates and thus microbial transformation of plant structural inputs and therefore POM accumulation.

Chemical diversity was a lower predictor of SOM stabilization efficiency than expected on the basis of the functional complexity hypotheses (Lehmann et al., 2020), and only in the subsoil linearly related to litter-derived C stabilization efficiency in POM (Fig. 9). POM is expected to accumulate in soil as a result of microbial inhibition or limitation to decomposition (Cotrufo and Lavallee 2021). Possibly the low microbial abundance and chemical complexity background of the subsoil may have resulted in a higher energetic demand on investment for the microbial decomposition of input residues and POM, resulting in their accumulation (Lehmann et al., 2020), compared to the topsoil characterized by higher microbial abundance and soil chemical complexity backgrounds. By contrast, the effect of microbial diversity varied across soils and SOM fractions: it was positively related to stabilization efficiencies in POM in both the topsoil and subsoil (Fig. 9), and negatively to the stabilization efficiency in MAOM in the topsoil (Fig. 10). Weak and inconsistent relationships of microbial diversity to SOM stabilization efficiencies have been previously observed (Ernakovich et al., 2021), and more mechanistic studies exploring these relationships across a variety of soils are warranted.

#### 4.4. Conclusions

Our laboratory incubation study indicated that the addition of fresh residues to soil is the most inefficient way to form SOM, both in MAOM and POM. Rather leaching of plant residues and the addition of leachates can result in efficient MAOM formation, likely because of direct sorption of the soluble compounds to minerals. On the other hand, partially decomposed plant residues can result in efficient POM formation, likely because of them increasing soil microbial diversity, and soil chemical diversity in SOM poor soils, such as subsoil. Our subsoil was characterized by lower microbial abundance and higher C saturation deficit than topsoil. Therefore, it had a higher inherent capacity to form SOM than topsoil, both because organic matter input mineralization was slower resulting in higher retention of input-derived C and N in undecomposed residues and POM, but also because of the higher sorption potential to form MAOM. These findings suggest that soil management for SOM accrual should promote the separate addition of decomposed residues, such as compost, and soluble plant inputs to soils with high C saturation deficit and low microbial abundance, conditions typically observed in subsoils.

#### Declaration of competing interest

The authors declare the following financial interests/personal relationships which may be considered as potential competing interests: M. Francesca Cotrufo reports a relationship with Cquester Analytics LLC that includes: board membership and equity or stocks. M. Francesca Cotrufo and Michelle Haddix are both cofounders of Cquester Analytics LLC, <https://www.cquesteranalytics.com/>

#### Acknowledgements

We thank Dr. John Dunbar for supporting this study. We also thank Miho Yoshioka for help with py-GC/MS analysis and data wrangling. This work was supported by the U.S. Department of Energy, Office of Science, Biological and Environmental Research Division (Award number F255LANL2018) and through a CSU-USDA-ARS collaboration agreement (number 58-3012-6-016).

#### Appendix A. Supplementary data

Supplementary data to this article can be found online at <https://doi.org/10.1016/j.soilbio.2022.108648>.

#### References

- Albright, M.B., Johansen, R., Thompson, J., Lopez, D., Gallegos-Graves, L.V., Kroeger, M.E., Runde, A., Mueller, R.C., Washburne, A., Munsky, B., 2020. Soil bacterial and fungal richness forecast patterns of early pine litter decomposition. *Frontiers in Microbiology* 11, 42220.
- Amundson, R., Berhe, A.A., Hopmans, J.W., Olson, C., Szein, A.E., Sparks, D.L., 2015. Soil and human security in the 21st century. *Science* 348, 1261071.
- Bani, A., Pioli, S., Ventura, M., Panzacchi, P., Borruso, L., Tognetti, R., Tonon, G., Brusetti, L., 2018. The role of microbial community in the decomposition of leaf litter and deadwood. *Applied Soil Ecology* 126, 75–84.
- Bates, S.T., Berg-Lyons, D., Caporaso, J.G., Walters, W.A., Knight, R., Fierer, N., 2010. Examining the global distribution of dominant archaeal populations in soil. *The ISME Journal* 5, 908.
- Berg, B., McClaugherty, C., 2008. *Plant Litter Decomposition, Humus Formation, Carbon Sequestration*. Springer, Berlin.
- Bonner, M.T.L., Shoo, L.P., Brackin, R., Schmidt, S., 2018. Relationship between microbial composition and substrate use efficiency in a tropical soil. *Geoderma* 315, 96–103.
- Boutton, T.W., 1996. Stable carbon isotope ratios of soil organic matter and their use as indicators of vegetation and climate change. In: Boutton, T.W., Yamasaki, S. (Eds.), *Mass Spectrometry of Soils*. Marcel Dekker, Inc., New York, pp. 47–82.
- Cambardella, C.A., Elliott, E.T., 1992. Particulate soil organic-matter changes across a grassland cultivation sequence. *Soil Science Society of America Journal* 56, 777–783.
- Castellano, M., Mueller, K., Olk, D., Sawyer, J., Six, J., 2015. Integrating plant litter quality, soil organic matter stabilization and the carbon saturation concept. *Global Change Biology* 21, 3200–3209.
- Chen, S., Martin, M.P., Saby, N.P.A., Walter, C., Angers, D.A., Arrouays, D., 2018. Fine resolution map of top- and subsoil carbon sequestration potential in France. *The Science of the Total Environment* 630, 389–400.
- Christensen, B.T., 2001. Physical fractionation of soil and structural and functional complexity in organic matter turnover. *European Journal of Soil Science* 52, 345–353.
- Collins, H., Elliott, E., Paustian, K., Bundy, L., Dick, W., Huggins, D., Smucker, A., Paul, E., 2000. Soil carbon pools and fluxes in long-term corn belt agroecosystems. *Soil Biology and Biochemistry* 32, 157–168.
- Córdova, S.C., Olk, D.C., Dietzel, R.N., Mueller, K.E., Archontoulis, S.V., Castellano, M.J., 2018. Plant litter quality affects the accumulation rate, composition, and stability of mineral-associated soil organic matter. *Soil Biology and Biochemistry* 125, 115–124.
- Cotrufo, M.F., Lavallee, J., 2021. Soil organic matter formation, persistence and functioning: a synthesis of current understanding to inform its conservation and regeneration. *Advances in Agronomy* 172, 1–50.
- Cotrufo, M.F., Ranalli, M.G., Haddix, M.L., Six, J., Lugato, E., 2019. Soil carbon storage informed by particulate and mineral-associated organic matter. *Nature Geoscience* 12, 989–994.
- Cotrufo, M.F., Soong, J.L., Horton, A.J., Campbell, E.E., Haddix, M.H., Wall, D.L., Paustian, W.J., 2015. Soil organic matter formation from biochemical and physical pathways of litter mass loss. *Nature Geoscience* 8, 776–779.
- Cotrufo, M.F., Wallenstein, M., Boot, M.C., Denef, K., Paul, E.A., 2013. The Microbial Efficiency-Matrix Stabilization (MEMS) framework integrates plant litter decomposition with soil organic matter stabilization: do labile plant inputs form stable soil organic matter? *Global Change Biology* 19, 988–995.
- Davidson, E.A., Swank, W.T., 1986. Environmental parameters regulating gaseous nitrogen losses from two forested ecosystems via nitrification and denitrification. *Applied and Environmental Microbiology* 52, 1287–1292.
- Domeignoz-Horta, L.A., Shinjuku, M., Junier, P., Poirier, S., Verrecchia, E., Sebag, D., DeAngelis, K.M., 2021. The role of microbial diversity in the formation of soil organic matter quality and persistence. *bioRxiv* 23, 441131, 04.
- Ekschmitt, K., Kandeler, E., Poll, C., Brune, A., Buscot, F., Friedrich, M., Gleixner, G., Hartmann, A., Kastner, M., Marhan, S., Miltner, A., Scheu, S., Wolters, V., 2008. Soil-carbon preservation through habitat constraints and biological limitations on decomposer activity. *Journal of Plant Nutrition and Soil Science* 171, 27–35.
- Ernakovich, J.G., Baldock, J., Creamer, C., Sanderman, J., Kalbitz, K., Farrell, M., 2021. A combined microbial and ecosystem metric of carbon retention efficiency explains land cover-dependent soil microbial biodiversity–ecosystem function relationships. *Biogeochemistry* 153, 1–15.
- Fox, J., Weisberg, S., 2019. *TETO & sage., C. An {R} Companion to Applied Regression*, third ed. Thousand Oaks. CA: Sage.
- Fulton-Smith, S., Cotrufo, M.F., 2019. Pathways of soil organic matter formation from above and belowground inputs in a Sorghum bicolor bioenergy crop. *Global Change Biology Bioengineering* 11, 1–17.
- Gloor, G.B., Hummelen, R., Macklaim, J.M., Dickson, R.J., Fernandes, A.D., MacPhee, R., Reid, G., 2010. Microbiome profiling by illumina sequencing of combinatorial sequence-tagged PCR Products. *PLoS One* 5, e15406.
- Goering, H.K., Van Soest, P.J., 1970. Forage fiber analyses (apparatus, reagents, procedures, and some applications). *U.S. Agric. Res. Serv.* 379, 1–22.

- Grandy, A.S., Neff, J.C., 2008. Molecular C dynamics downstream: the biochemical decomposition sequence and its impact on soil organic matter structure and function. *The Science of the Total Environment* 404, 297–307.
- Gray, C.M., Monsom, R.K., Fierer, N., 2010. Emissions of volatile organic compounds during the decomposition of plant litter. *Journal of Geophysical Research: Biogeosciences* 115, G03015.
- Guenet, B., Gabrielle, B., Chenou, C., Arrouays, D., Balesdent, J., Bernoux, M., Bruni, E., Caliman, J.P., Cardinael, R., Chen, S., Ciais, P., 2021. Can  $\text{N}_2\text{O}$  emissions offset the benefits from soil organic carbon storage? *Global Change Biology* 27, 237–256.
- Haddix, M.H., Paul, E., Cotrufo, M.F., 2016. Dual, differential isotope labeling shows the preferential movement of labile plant carbon into mineral-bonded soil organic matter. *Global Change Biology Bioenergy* 22, 2301–2312.
- Haddix, M.L., Gregorich, E.G., Helgason, B.L., Janzen, H., Ellert, B.H., Cotrufo, M.F., 2020. Climate, carbon content, and soil texture control the independent formation and persistence of particulate and mineral-associated organic matter in soil. *Geoderma* 363, 114160.
- Heckman, K., Hicks Pries, C.E., Lawrence, C.R., Rasmussen, C., Crow, S.E., Hoyt, A.M., von Fromm, S.F., Shi, Z., Stoner, S., McGrath, C., Beem-Miller, J., Berhe, A.A., Blankinship, J.C., Keiluweit, M., Marin-Spiotta, E., Monroe, J.G., Plante, A.F., Schimel, J., Sierra, C.A., Thompson, A., Wagai, R., 2021. Beyond bulk: density fractions explain heterogeneity in global soil carbon abundance and persistence. *Global Change Biology* 1–19, 00.
- Hutchinson, M.I., Bell, T.A., Dunbar, J., Albright, M., 2021. Merging fungal and bacterial community profiles via an internal control. *Microbial Ecology* 82, 484–497.
- Kallenbach, C.M., Frey, S.D., Grandy, A.S., 2016. Direct evidence for microbial-derived soil organic matter formation and its ecophysiological controls. *Nature Communications* 7, 13630.
- Keesstra, S.D., Bouma, J., Wallinga, J., Tittonell, P., Smith, P., Cerdà, A., Montanarella, L., Quinton, J.N., Pachepsky, Y., van der Putten, W.H., Bardgett, R.D., Moolenaar, S., Mol, G., Jansen, B., Fresco, L.O., 2016. The significance of soils and soil science towards realization of the United Nations Sustainable Development Goals. *Soil* 2, 111–128.
- Kleber, M., Eusterhues, K., Keiluweit, M., Mikutta, C., Mikutta, R., Nico, P.S., 2015. Mineral-organic associations: formation, properties, and relevance in soil environments. *Advances in Agronomy* 130, 1–140.
- Lavallee, J.M., Conant, R.T., Paul, E.A., Cotrufo, M.F., 2018. Incorporation of shoot versus root-derived  $^{13}\text{C}$  and  $^{15}\text{N}$  into mineral-associated organic matter fractions: results of a soil slurry incubation with dual-labelled plant material. *Biogeochemistry* 137, 379–393.
- Lavallee, J.M., Soong, J.L., Cotrufo, M.F., 2020. Conceptualizing soil organic matter into particulate and mineral-associated forms to address global change in the 21<sup>st</sup> century. *Global Change Biology* 26, 261–273.
- Lehmann, J., Hansel, C.M., Kaiser, C., Kleber, M., Maher, K., Manzoni, S., Nunan, N., Reichstein, M., Schimel, J.P., Torn, M.S., 2020. Persistence of soil organic carbon caused by functional complexity. *Nature Geoscience* 13, 529–534.
- Lehmann, J., Kleber, M., 2015. The contentious nature of soil organic matter. *Nature* 528, 60–68.
- Leichty, S., Cotrufo, M.F., Stewart, C.E., 2020. Less efficient residue-derived soil organic carbon formation under no-till irrigated corn. *Soil Science Society of America Journal* 84, 1928–1942.
- Liang, C., Schimel, J.P., Jastrow, J.D., 2017. The importance of anabolism in microbial control over soil carbon storage. *Nature Microbiology* 2, 17105.
- Linn, D.M., Doran, J.W., 1984. Effect of water-filled pore space on carbon dioxide and nitrous oxide production in tilled and nontilled soils. *Soil Science Society of America Journal* 48, 1267–1272.
- Lugato, E., Lavallee, J.M., Haddix, M.L., Panagos, P., Cotrufo, M.F., 2021. Different climate sensitivity of particulate and mineral-associated soil organic matter. *Nature Geoscience* 14, 295–300.
- Lynch, L.M., Machmuller, M.B., Cotrufo, M.F., Paul, E.A., Wallenstein, M.D., 2018. Tracking the fate of fresh carbon in the Arctic tundra: will shrub expansion alter responses of soil organic matter to warming? *Soil Biology and Biochemistry* 120, 134–144.
- Malik, A.A., Chowdhury, S., Schlager, V., Oliver, A., Puissant, J., Vazquez, P.G., Jehmlich, N., von Bergen, M., Griffiths, R.I., Gleixner, G., 2016. Soil fungal: bacterial ratios are linked to altered carbon cycling. *Frontiers in Microbiology* 7, 1247.
- McKee, G.A., Soong, J., Calderon, F., Borch, T., Cotrufo, M.F., 2016. An integrated spectroscopic and wet chemical approach to investigate grass litter decomposition chemistry. *Biogeochemistry* 128, 107–123.
- McMurdie, P.J., Holmes, S., 2013. phyloseq: an R package for reproducible interactive analysis and graphics of microbiome census data. *PLoS One* 8 (4), e61217.
- Mitchell, E., Scheer, C., Rowlings, D., Conant, R.T., Cotrufo, M.F., Grace, P., 2018. Amount and incorporation of plant residue inputs modify residue stabilisation dynamics in soil organic matter fractions. *Agriculture, Ecosystems & Environment* 256, 82–91.
- Mitchell, E., Scheer, C., Rowlings, D.W., Conant, R.T., Cotrufo, M.F., van Delden, L., Grace, P.R., 2016. The influence of above-ground residue input and incorporation on GHG fluxes and stable SOM formation in a sandy soil. *Soil Biology and Biochemistry* 101, 104–113.
- Mosier, S., Apfelbaum, S., Byck, P., Calderon, F., Teague, R., Thompson, R., Cotrufo, M.F., 2021. Adaptive multi-paddock grazing enhances soil carbon and nitrogen stocks and stabilization through mineral association in southeastern US grazing lands. *Journal of Environmental Management* 288, 112409.
- Mueller, R., Belnap, J., Kuske, C., 2015. Soil bacterial and fungal community responses to nitrogen addition across soil depth and microhabitat in an arid shrubland. *Frontiers in Microbiology* 6, 891.
- Mueller, R.C., Gallegos-Graves, L.V., Kuske, C.R., 2016. A new fungal large subunit ribosomal RNA primer for high-throughput sequencing surveys. *FEMS Microbiology Ecology* 92, fiv153.
- Preston, C.M., Trofymow, J.A., 2015. The chemistry of some foliar litters and their sequential proximate analysis fractions. *Biogeochemistry* 126, 197–209.
- R Core Group, 2019. R: A language and environment for statistical computing. R Foundation for Statistical Computing, Vienna, Austria. <https://www.R-project.org/>.
- Rocci, K.S., Lavallee, J.M., Stewart, C., Cotrufo, M.F., 2021. Soil organic carbon response to global environmental change depends on its distribution between mineral-associated and particulate organic matter: a meta-analysis. *The Science of the Total Environment* 793, 148569.
- Samson, M.-É., Chantigny, M.H., Vanasse, A., Menasseri-Aubry, S., Angers, D.A., 2020. Coarse mineral-associated organic matter is a pivotal fraction for SOM formation and is sensitive to the quality of organic inputs. *Soil Biology and Biochemistry* 149, 107935.
- Sanderman, J., Hengl, T., Fiske, G.J., 2017. Soil carbon debt of 12,000 years of human land use. *Proceedings of the National Academy of Sciences* 114, 9575–9580.
- Sanderman, J., Maddern, T., Baldock, J., 2014. Similar composition but differential stability of mineral retained organic matter across four classes of clay minerals. *Biogeochemistry* 121, 409–424.
- Six, J., Conant, R.T., Paul, E.A., Paustian, K., 2002. Stabilization mechanisms of soil organic matter: implications for C-saturation of soils. *Plant and Soil* 241, 155–176.
- Six, J., Frey, S.D., Thiet, R.K., Batten, K.M., 2006. Bacterial and fungal contributions to carbon sequestration in agroecosystems. *Soil Science Society of America Journal* 70, 555–569.
- Smith, P., Cotrufo, M.F., Rumpel, C., Paustian, K., Kuikman, P., Elliott, J., McDowell, R., Griffiths, R., Asakawa, S., Bustamante, M., 2015. Biogeochemical cycles and biodiversity as key drivers of ecosystem services provided by soils. *Soil* 1, 665–685.
- Sokol, N.W., Sanderman, J., Bradford, M.A., 2019. Pathways of mineral-associated soil organic matter formation: integrating the role of plant carbon source, chemistry, and point of entry. *Global Change Biology* 25, 12–24.
- Soong, J.L., Parton, W.J., Calderon, F.J., Campbell, N., Cotrufo, M.F., 2015. A new conceptual model on the fate and controls of fresh and pyrolyzed plant litter decomposition. *Biogeochemistry* 124, 27–44.
- Stewart, C.E., 2012. Evaluation of angiosperm and fern contributions to soil organic matter using two methods of pyrolysis-gas chromatography-mass spectrometry. *Plant and Soil* 351, 31–46.
- Stewart, C.E., Follett, R.F., Pruessner, E.G., Varvel, G.E., Vogel, K.P., Mitchell, R.B., 2016. N fertilizer and harvest impacts on bioenergy crop contributions to SOC. *Global Change Biology Bioenergy* 8, 1201–1211.
- Stewart, C.E., Paustian, K., Conant, R.T., Plante, A.F., Six, J., 2007. Soil carbon saturation: concept, evidence and evaluation. *Biogeochemistry* 86, 19–31.
- Stewart, C.E., Paustian, K., Conant, R.T., Plante, A.F., Six, J., 2008. Soil carbon saturation: evaluation and corroboration by long-term incubations. *Soil Biology and Biochemistry* 40, 1741–1750.
- Stewart, C.E., Plante, A.F., Paustian, K., Conant, R.T., Six, J., 2008b. Soil carbon saturation: linking concept and measurable carbon pools. *Soil Science Society of America Journal* 72, 379–392.
- Strickland, M.S., Wickings, K., Bradford, M.A., 2012. The fate of glucose, a low molecular weight compound of root exudates, in the belowground foodweb of forests and pastures. *Soil Biology and Biochemistry* 49, 23–29.
- Talbot, J.M., Bruns, T.D., Taylor, J.W., Smith, D.P., Branco, S., Glassman, S.I., Erlandsen, S., Vilgalys, R., Liao, H.-L., Smith, M.E., Peay, K.G., 2014. Endemism and functional convergence across the North American soil mycobiome. *Proceeding of the National Academy of Sciences* 111, 6341–6346.
- Taylor, J.P., Wilson, B., Mills, M.S., Burns, R.G., 2002. Comparison of microbial numbers and enzymatic activities in surface soils and subsoils using various techniques. *Soil Biology and Biochemistry* 34, 387–401.
- von Lutzow, M., Kogel-Knabner, I., Ekschmitt, K., Matzner, E., Guggenberger, G., Marschner, B., Flessa, H., 2006. Stabilization of organic matter in temperate soils: mechanisms and their relevance under different soil conditions - a review. *European Journal of Soil Science* 57, 426–445.
- Zhang, Y., Lavallee, J.M., Robertson, A.D., Even, R., Ogle, S.M., Paustian, K., Cotrufo, M.F., 2021. Simulating measurable ecosystem carbon and nitrogen dynamics with the mechanically-defined MEMS 2.0 model. *Biogeoosciences* 18, 3147–3171.

# The role of plant input physical-chemical properties, and microbial and soil chemical diversity on the formation of particulate and mineral-associated organic matter

Cotrufo, M. Francesca; Haddix, Michelle L.; Kroeger, Marie E.; Stewart, Catherine E.

01 mingxi zhang

Page 2

8/8/2023 8:17